MATERIALS SCIENCE

Solar-assisted fabrication of large-scale, patternable transparent wood

Qinqin Xia*, Chaoji Chen*, Tian Li, Shuaiming He, Jinlong Gao, Xizheng Wang, Liangbing Hu†

Transparent wood is considered a promising structural and light management material for energy-efficient engineering applications. However, the solution-based delignification process that is used to fabricate transparent wood generally consumes large amounts of chemicals and energy. Here, we report a method to produce optically transparent wood by modifying the wood's lignin structure using a solar-assisted chemical brushing approach. This method preserves most of the lignin to act as a binder, providing a robust wood scaffold for polymer infiltration while greatly reducing the chemical and energy consumption as well as processing time. The obtained transparent wood (~1 mm in thickness) demonstrates a high transmittance (>90%), high haze (>60%), and excellent light-guiding effect over visible wavelength. Furthermore, we can achieve diverse patterns directly on wood surfaces using this approach, which endows transparent wood with excellent patternability. Combining its efficient, patternable, and scalable production, this transparent wood is a promising candidate for applications in energy-efficient buildings.

INTRODUCTION

The growing demand of optical components in energy-efficient buildings (*1*–*3*), optoelectronics (*4*–*6*), solar cells (*7*), and solar desalination devices (*8*) has fueled the search for high-performance, sustainable optical materials. Toward this aim, transparent wood has emerged due to its unique hierarchical structure (*9*–*10*), high specific strength (*11*–*12*), and favorable light management properties (*13*–*14*), demonstrating a broad range of applications including optoelectronic devices (*15*–*18*), energy-efficient building materials (*9*, *19*–*20*), light management layers for solar cells (*21*–*22*), and touch panels (*23*–*24*). To fabricate transparent wood, two steps are typically involved: (i) completely removing the light-absorbing lignin from the cell walls of natural wood by a solution-based immersion method and (ii) infiltrating a refractive index matching polymer into the delignified wood matrix to minimize light absorption and scattering, respectively (*9*, *13*, *25*–*27*). However, this solution-based delignification process impairs the mechanical strength of wood and is also relatively energy and chemical intensive. Furthermore, it is necessary to fully remove the dispersed lignin from the wood scaffold, which lengthens the processing time (6 to 12 hours) (*9*–*10*, *18*, *28*–*29*). Last, the generated liquid waste is difficult to recycle and creates an additional environmental burden.

To address these processing issues as well as obtain desirable optical and mechanical properties, recent studies have begun to optimize the preparation of transparent wood by controlling the degree of delignification. For example, Qin *et al.* (*30*) prepared a laminated transparent wood of 1.5 mm in thickness (~82% optical transmittance) using a two-step partial delignification method ($NaClO_2$/H_2O_2), in which 80% of lignin was removed and the processing time was reduced to 3 hours. Meanwhile, Wu *et al.* (*31*) prepared a transparent wood (~61% optical transmittance) from basswood (0.42 mm in thickness) with improved mechanical properties by reducing the degree of delignification (75% lignin content was removed) using a $NaClO_2$ solution method. Although these partial delignification methods reduce the processing time and improve the mechanical characteristics of transparent wood, they require toxic chemicals that are difficult to dispose, as well as large solution volumes to enable complete immersion of the materials. In addition, further simplifying the reaction process with even shorter processing time would improve the scalability and efficiency of transparent wood production.

We note that the chromophore groups in lignin are mainly responsible for the brownish color and light absorption properties of natural wood (*32*). Recently, researchers have found that lignin can be decolored by altering the chromophoric composition (*33*–*36*) rather than removing the lignin structure entirely. For example, Li *et al.* (*36*) reported a transparent wood that retained its lignin content and instead removed the lignin chromophore using an alkaline H_2O_2 hydrothermal solution to reduce the processing time. H_2O_2 as a desirable oxidant produces only water as a by-product, which notably reduces the waste liquid production. However, like previous techniques, this method requires relatively large chemical, water, and energy consumption. Therefore, it has remained challenging to process transparent wood in a fast, scalable, low cost, and environmentally friendly way.

Here, we report on a technique for rapidly fabricating transparent wood that involves chemical brushing, rather than immersion, combined with solar illumination to remove the lignin chromophore. Figure 1A shows the fabrication process of the transparent wood via a two-step approach. First, we modify the lignin structure by brushing H_2O_2 across the wood surface, followed by ultraviolet (UV) light illumination that can be conducted using natural sunlight to remove the light-absorbing chromophores of lignin. Refractive index matching epoxy can then be easily infiltrated into the microporous wood structure to prepare the transparent wood, which features a dense microstructure and low light scattering. The hierarchically porous structure of natural wood promotes fast H_2O_2 solution infiltration/diffusion and UV light trapping to efficiently remove the light-absorbing chromophore of lignin, significantly reducing its light absorption (<4%). Compared to lignin-removed wood (0.4 MPa), the lignin-modified wood also shows a substantially higher tensile strength (20.6 MPa) due to the presence of the modified lignin

Department of Materials Science and Engineering, University of Maryland, College Park, MD 20742, USA.
*These authors contributed equally to this work.
†Corresponding author. Email: binghu@umd.edu

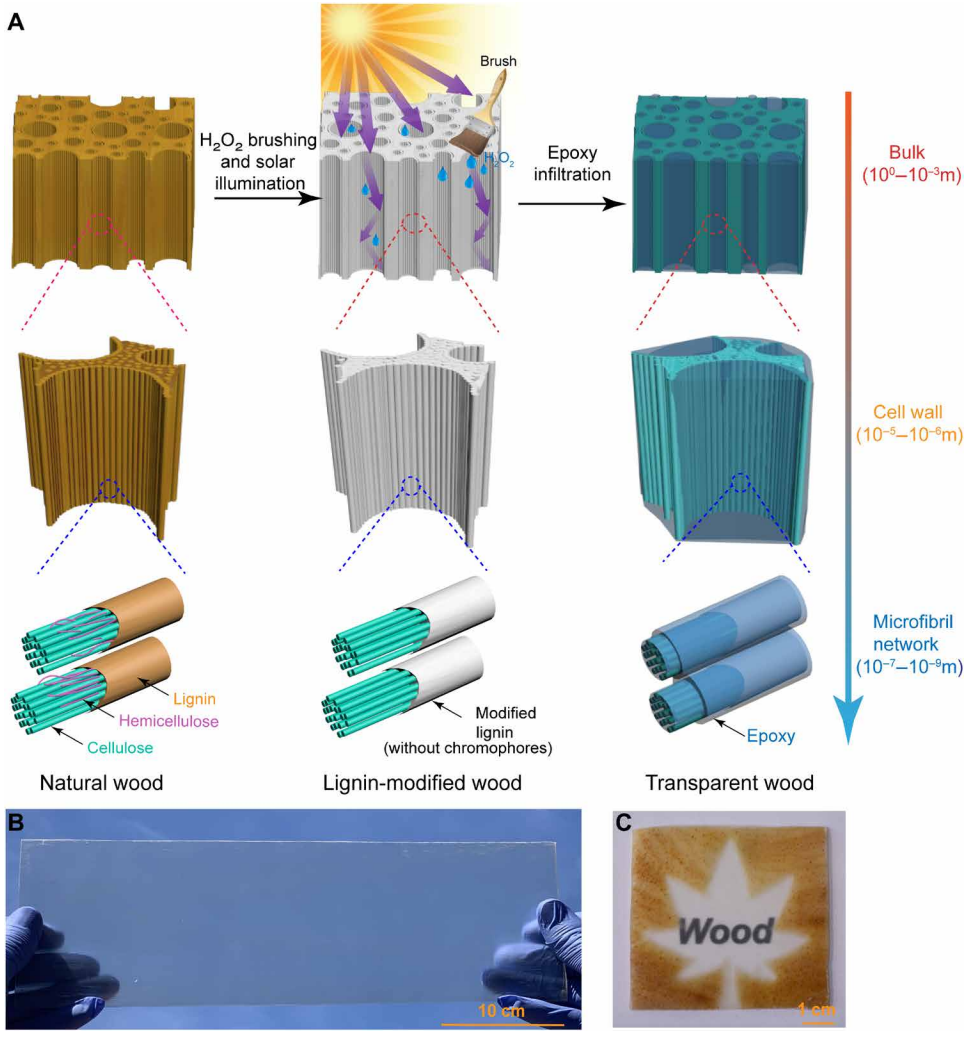

Fig. 1. Schematic illustration of fabricating transparent wood and demonstration of its patterning. (**A**) Schematic illustration of this simple yet effective, eco-friendly, scalable, and low-cost method of fabricating transparent wood. Lignin not only endows natural wood with a brownish color but also serves as a binder for cellulose and hemicellulose. After chemical brushing and solar illumination, the lignin chromophore and hemicellulose are removed and the natural wood becomes colorless, but the modified lignin remains and can still effectively bind and wrap around the cellulose microfibrils to maintain the material's mechanical properties. Then, epoxy can be easily infiltrated into the loosely packed lignin-modified wood microchannels to prepare the final transparent wood. (**B**) A digital image of a large-scale sheet of transparent wood (400 mm by 110 mm by 1 mm) along the longitudinal direction (i.e., the fiber direction). (**C**) A digital image of the transparent wood along the transverse direction (i.e., perpendicular to the fiber direction) patterned with a "tree leaf" shape. Photo credit: Qinqin Xia, University of Maryland, College Park.

binding with the well-oriented cellulose fibrils, which provides a strong and robust scaffold for polymer infiltration. Note that transparent wood can be made from both transversely and longitudinally cut natural wood, respectively (Fig. 1, B and C). The resulting transparent wood exhibits a high transmittance (up to ~90%), excellent tensile strength (> 46 MP), and favorable light guiding effect. In addition, the transparent wood can be easily patterned (Fig. 1C) using this chemical brushing combined with UV light illumination method. Compared with traditional solution-based immersion processes, our method requires fewer chemicals and energy consumptions, thus greatly reducing the preparation cost and liquid waste. This environmentally friendly, scalable, patternable, and low-cost transparent wood with favorable optical and mechanical properties holds great potential in energy-efficient building applications and light management devices.

RESULTS AND DISCUSSION

Preparation of transparent wood and its structural characteristics

Figure S1 shows the preparation process of transparent wood via this simple yet effective approach. First, ~15 ml of H_2O_2 [30 weight % (wt %) concentration] was brushed on a natural balsa wood sample (200 mm by 10 mm by 0.6 mm), followed by exposure to UV light (a UV lamp was used as the solar UV light simulator) for 1 hour until the natural wood color turned completely white. The resulting lignin-modified wood displays a low absorptivity (<4%) (fig. S2) and a high reflectivity (>88%) (fig. S3) in the range of 400 to 800 nm, suggesting the removal of the light-absorbing chromophores in lignin. Meanwhile, in the Fourier transform infrared (FTIR) spectrum of the lignin-modified wood, we attribute the absorption peaks at approximately 1595, 1505, and 1435 cm^{-1} to the aromatic vibrations

of lignin (Fig. 2A) (*37*–*38*), indicating that the process preserves the aromatic backbone of lignin despite degrading its chromophore. The peak of 1734 cm^{-1} is assigned to the carboxyl groups in hemicellulose (xylan/glucomannan). The peak of 1235 cm^{-1} belongs to the uronic acid groups of the hemicellulose or the ester linkage of the carboxyl groups of lignin and hemicellulose (*18*, *25*, *39*). The disappearance of 1734 cm^{-1} peak and the decrease of peak intensity of 1235 cm^{-1} in lignin-modified wood indicate the partial dissolution/removal of hemicellulose from natural wood after treatment. In addition, the lignin content of the natural wood and lignin-modified wood samples was ~23.5 and ~19.9%, respectively (Fig. 2B), which further suggests that the most of lignin structure was well preserved after the treatment.

We note that the preserved lignin can act as a binder to strengthen the mechanical properties of the lignin-modified wood as well as provide a robust wood scaffold for subsequent polymer infiltration (*40*–*41*). The lignin-modified wood exhibits a tensile strength of 20.6 MPa under wet conditions, which is ~50 times higher than lignin-removed wood (0.4 MPa) prepared by the traditional $NaClO_2$ solvent–based method (fig. S4). In addition, the lignin-modified wood shows excellent flexibility along the longitudinal (parallel to the fiber direction, L) and transverse directions (perpendicular to the fiber direction, T) (fig. S5). In contrast, the lignin-removed wood prepared by the traditional $NaClO_2$ solvent–based method is very fragile and easily cracked (fig. S6). Benefitting from the strong mechanical properties, we further prepared a large lignin-modified wood sample with a length of ~1 m using this chemical brushing combined with UV light illumination method (Fig. 2C).

Using this lignin-modified wood, we then infiltrated it with epoxy by vacuum to obtain the final transparent wood product. Figure 2 (D to I) shows scanning electron microscopy (SEM) images of the natural wood, lignin-modified wood, and transparent wood. The natural wood shows a three-dimensional hierarchical and interconnected porous structure (Fig. 2, D and G, and fig. S7), featuring microchannels with diameters that range from ~15 to 300 μm. This unique porous structure is beneficial for fast H_2O_2 solution infiltration/diffusion and efficient UV light trapping inside the wood microchannels, which allows us to achieve efficient removal of light-absorbing chromophores during the process (fig. S8). Meanwhile, the diameters of the microchannels in the lignin-modified wood range from 10 to 270 μm (Fig. 2, E and H), demonstrating that lignin-modified wood preserves the hierarchical, interconnected porous structure after treatment. Last, SEM images of the transparent wood show the epoxy is well infiltrated into the pores of the lignin-modified wood (Fig. 2, F and I, and fig. S9). A dense and compact structure is formed in the transparent wood after the infiltration, which helps suppress light scattering and improves the optical transmittance (*11*, *14*).

The optical and mechanical performance of transparent wood

Transparent wood along T and L directions exhibits excellent optical properties. Images of the transparent wood in the L (Fig. 3A)

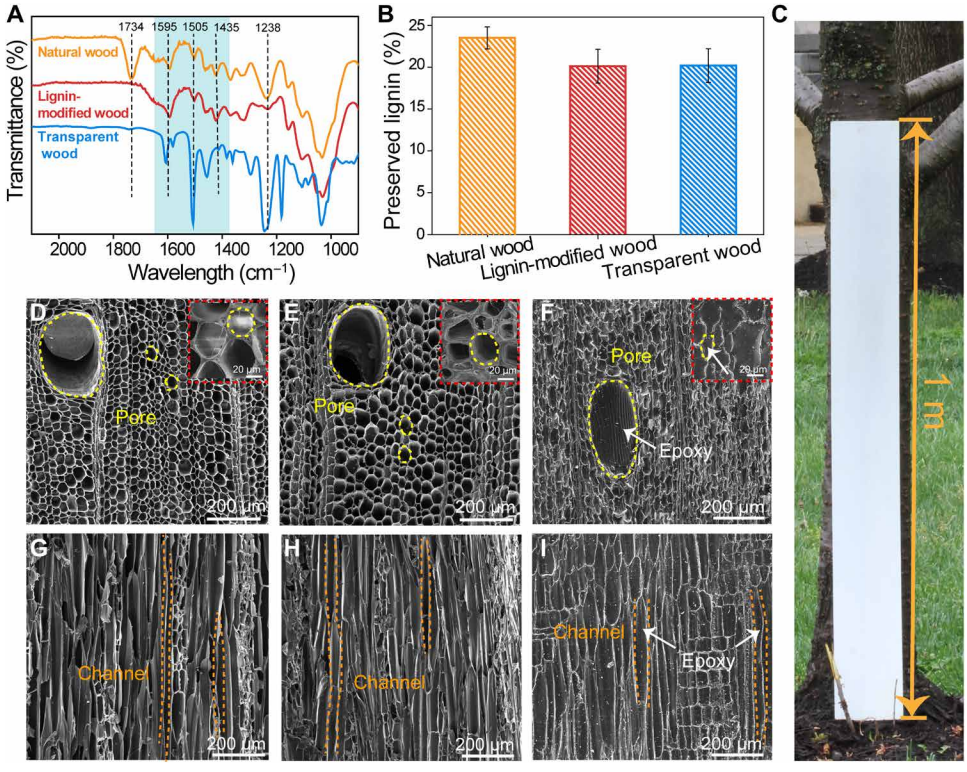

Fig. 2. Structural and compositional characterization of the transparent wood. (**A**) The FTIR spectra and (**B**) the preserved lignin content of the natural wood, lignin-modified wood, and transparent wood. (**C**) A digital image showing the meter-scale fabrication of lignin-modified wood based on our method. Scanning electron microscopy (SEM) images of the transverse direction of (**D**) natural wood, (**E**) lignin-modified wood, and (**F**) transparent wood. The insets in the magnified SEM images show a detailed view of the micropores in the samples. SEM images of the longitudinal direction of (**G**) natural wood, (**H**) lignin-modified wood, and (**I**) transparent wood. The thickness of samples is 1 mm. Photo credit: Qinqin Xia, University of Maryland, College Park.

and T directions (Fig. 3B) are demonstrated, in which we can clearly see the background through the materials. In addition, we can facilely prepare thick transparent wood (L, 1.5 mm; T, 3.5 mm) with the excellent optical transparency using chemical brushing combined with UV light illumination method (figs. S10 and S11). We measured the optical transmittance of the natural wood and transparent wood from 200 to 2000 nm (Fig. 3C). The transparent wood along the L and T directions has a high optical transmittance of ~90% over the visible wavelength range (400 to 800 nm) compared to the transmittance of the natural wood (L < 6%, T < 36%). The absorptivity of the transparent wood (near 0%) is also much lower than that of the natural wood (L < 83%) in visible wavelengths (Fig. 3D) due to the removal of the light-absorbing chromophore of lignin, which allows almost all visible light to pass through the transparent wood. Figure S12 shows the transparent wood exhibits a high transmittance haze of ~60 to 80% over the wavelength range of 400 to 800 nm. Transparent wood with excellent optical transparency can also be made from other wood species with different density, such as oak and poplar, suggesting the universality of this approach (fig. S13). In addition, the transparent wood features preserved vertically aligned microchannels, which allow light propagation to be guided along the channel direction. As shown in Fig. 3E, we used a 650-nm red single mode laser to perpendicularly illuminate the transparent wood along the L and T directions. Our results show the beam propagates along the direction of the wood channels, indicating the transparent wood has light guiding capacity and anisotropic optical transmittance (*10*, *14*, *42*–*43*).

We measured the mechanical properties of the natural wood and transparent wood at different tensile directions. The tensile strengths of the natural wood (stress along the L and T directions) were 24.5 and 0.7 MPa, respectively (Fig. 3F). Meanwhile, the tensile strengths of the L- and T-transparent wood samples were 46.2 and 31.4 MPa, respectively, which corresponds to an enhancement of 1.8 times and 44.8 times higher than the natural wood (L and T). The L- and T-transparent wood also have a significantly improved toughness of 0.93 and 1.64 MJ m^{-3} compared to the natural wood (L, 0.26 MJ m^{-3}; T, 0.03 MJ m^{-3}), as shown in Fig. 3G. The toughness of the L-transparent wood is lower than that of the T-transparent wood because of the smaller elongation at break of the L-sample (3.4% < 7.4%) (Fig. 3F). We attribute the improved mechanical strength of the transparent wood to its lignin-reinforced anisotropic structure as well as the infiltrated epoxy, the tensile strength of which is ~87 MPa (fig. S14). In addition, the low volume fraction of wood scaffold also contributes to the improved mechanical properties of transparent wood (fig. S15). Benefiting from the high mechanical strength, the transparent wood is also quite flexible (fig. S16). The transparent wood has both excellent optical properties (high optical transmittance, high haze, and light guiding effect) and excellent mechanical strength, which suggest its application in energy-efficient buildings and light management devices.

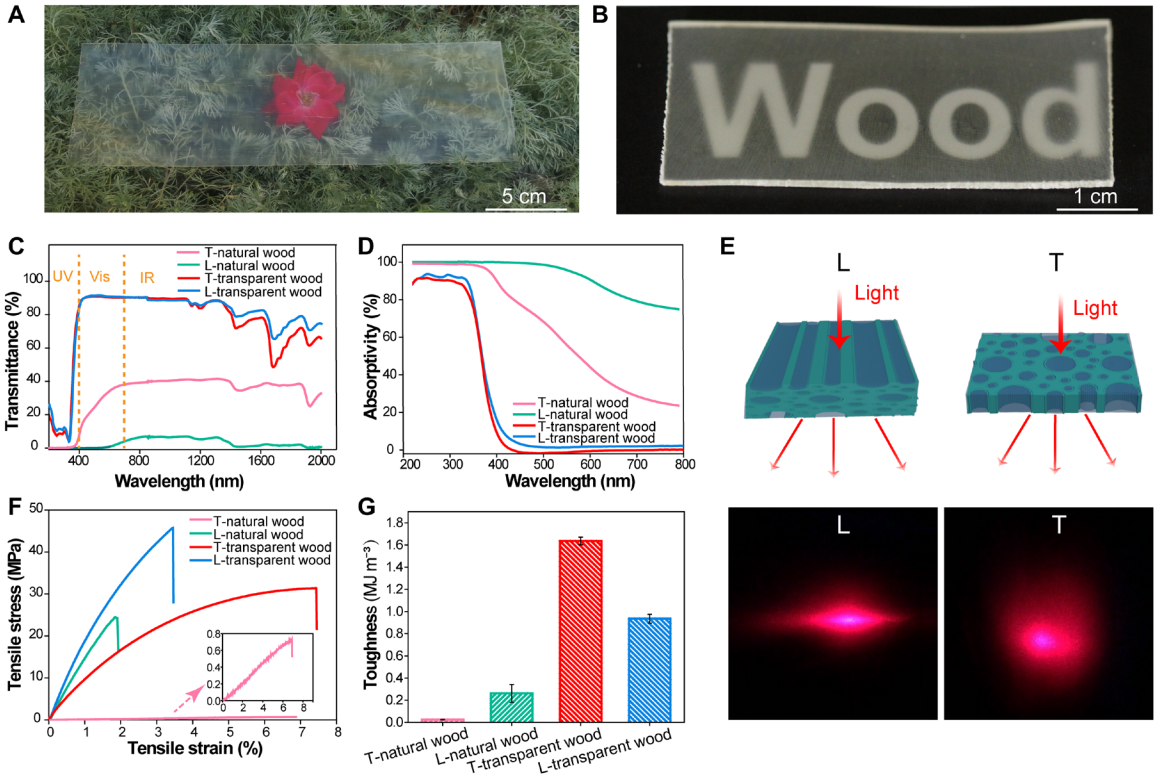

Fig. 3. The optical and mechanical properties of the natural wood and transparent wood. Digital images of the transparent wood along the (**A**) longitudinal direction (L; 400 mm by 110 mm by 1 mm) and (**B**) transverse direction (T; 70 mm by 30 mm by 1.5 mm). (**C**) The transmittance and (**D**) absorption of the natural wood and transparent wood (the volume fraction of lignin-modified wood scaffold: L, ~30%; T, ~33.2%). (**E**) Guided light propagation by the transparent wood. Photo images of the scattered laser light spot of the L- and T-transparent wood materials. (**F**) The tensile strength and (**G**) toughness of the natural wood and transparent wood. Photo credit: Qinqin Xia, University of Maryland, College Park.

Optically transparent wood with excellent patternability

Traditional solution-based delignification methods generally involve entirely immersing the wood samples in chemical solutions, which makes it difficult to bleach selective areas of the material. In contrast, our chemical brushing combined with UV light illumination method allows us to selectively bleach designated areas of the wood samples, which enables us to easily prepare transparent wood with diverse patterns (movie S1). The transparent wood can be selectively and precisely patterned by taking advantage of the different optical transmittance between natural wood (6 to 36%) and transparent wood (~90%), as shown in fig. S17. First, the desired patterns drawn with a brush on the natural wood samples using H_2O_2 as an were "ink." Then, these regions were illuminated with UV light, which turns them white. We then infiltrated epoxy into the microchannels of the lignin-modified wood to obtain transparent wood with desired patterns (Fig. 4, A and B, and fig. S18). T-transparent wood samples with number ("4") and letter ("A") patterns are shown in Fig. 4 (C and D). In this case, we wrote the number 4 in the brownish color of the natural wood, which was defined by the patterned transparent area, while the transparent letter A was patterned in the reverse. We also demonstrated L-transparent wood samples with more complex geometries, including two transparent circles minus a nontransparent diamond and a yin-yang symbol (Fig. 4, E and F), showing transparent wood with arbitrary patterns can be achieved using our chemical brushing combined with UV light illumination method. Figure 4 (C to F) shows that the patterned transparent wood can be made from transversely and longitudinally cut natural wood, respectively, suggesting the high versatility in direction selection and pattern designability of our method.

Demonstration of solar-assisted fabrication of transparent wood

UV light (100 to 400 nm) on Earth originates from the Sun (an inexhaustible source), with more than 95% of the wavelengths that reach the planet's surface being in the UVA range (315 to 400 nm) (*44*). Thus, we use this solar UV light as a driver of wood decoloration to achieve the rapid fabrication of transparent wood. The schematic diagram in Fig. 5A demonstrates the potential large-scale fabrication of transparent wood based on the mature rotary wood cutting method in wood industry and the solar-assisted chemical brushing process. The lignin-modified wood can be continuously and rapidly fabricated in this eco-friendly and energy-saving solar-driven manner for further scalable fabrication of transparent wood with high reliability and productivity. As shown in Fig. 5B, three large pieces of balsa wood with a length of 1 m can be rapidly produced in 1 hour by solar UV radiation [Global Solar UV Index: 7 to 8, Maryland, College Park (latitude: 39.00; longitude: −76.75) on 9 August 2019 at 13:00]. In our lab scale production, we obtained 400 mm by 110 mm by 1 mm of the transparent wood with high transmittance (Fig. 5C) after infiltrating epoxy into above lignin-modified wood.

We further evaluated the energy consumption, cost, and chemical emission of this production process for transparent wood and compared it with the $NaClO_2$ solution–based delignification methods (Fig. 5D). Our solar-assisted chemical brushing process only removes the chromophores of lignin and does not involve completely breaking the covalent bonds between cellulose and lignin. Thus, our method neither involves extensive usage of chemicals through harsh reaction nor high temperature treatment. Other solution-based methods generally require samples to be entirely

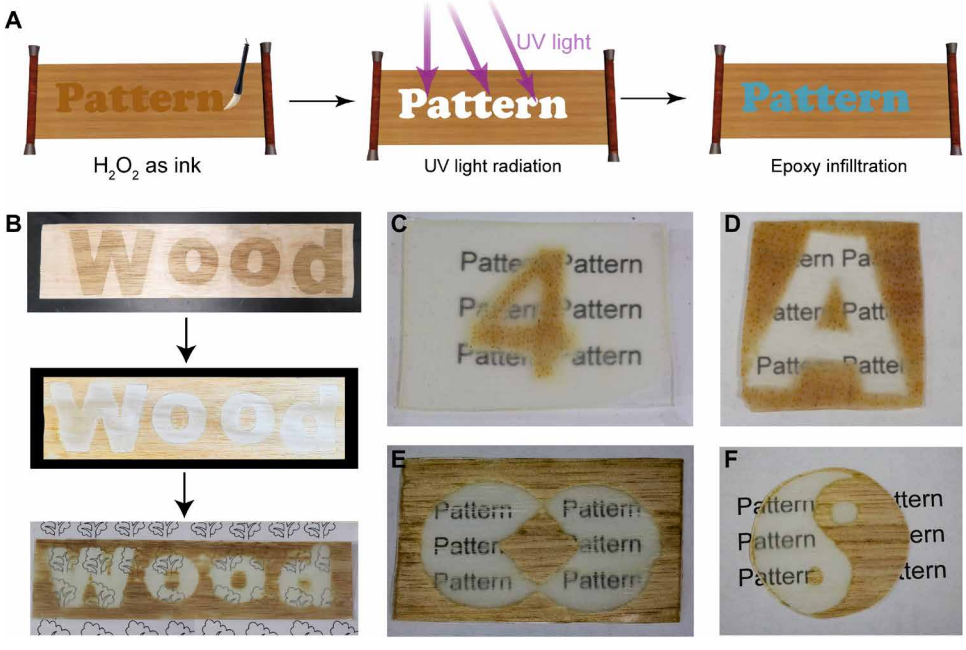

Fig. 4. The fabrication process of the patternable transparent wood. (**A**) Schematic and (**B**) experiments demonstrating the fabrication process of the patterned transparent wood. First, H_2O_2 ink is printed on the wood surface using a brush, and these areas turn white after UV illumination. After the infiltration of epoxy, transparent wood with different patterns can be obtained, with various patterns made from natural wood along the longitudinal and transverse directions. The transparent wood patterned with (**C**) the number 4 and (**D**) letter A. (**E**) Circle and diamond and (**F**) yin-yang patterned transparent wood samples. Photo credit: Qinqin Xia, University of Maryland, College Park.

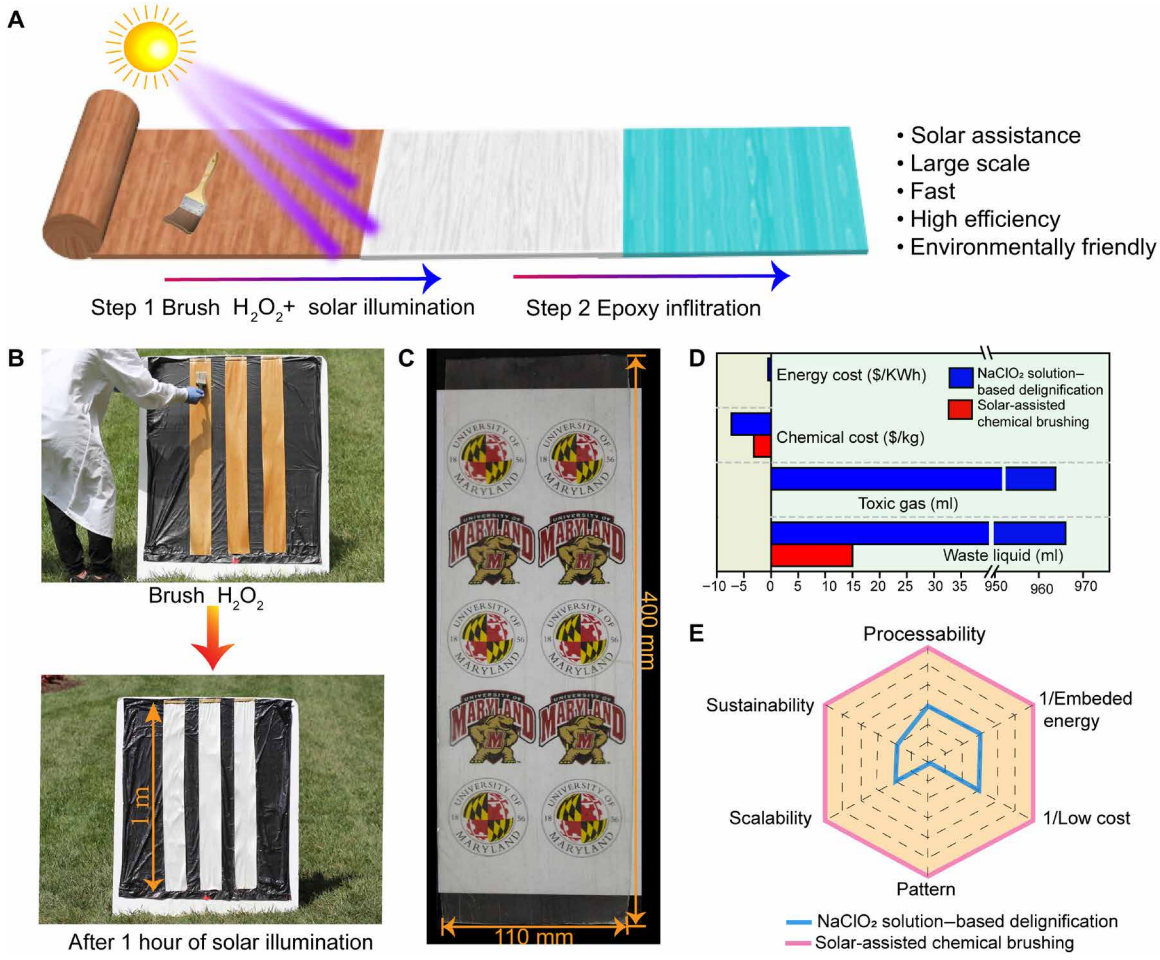

Fig. 5. Solar-assisted large-scale fabrication of transparent wood. (**A**) Schematic showing the potential large-scale fabrication of transparent wood based on the rotary wood cutting method and the solar-assisted chemical brushing process. (**B**) The outdoor fabrication of lignin-modified wood with a length of 1 m [9 August 2019 (the summer months) at 13:00 p.m. (solar noon), the Global Solar UV Index (UVI): 7 to 8]. (**C**) Digital photo of a piece of large transparent wood (400 mm by 110 mm by 1 mm). (**D**) The energy consumption, chemical cost, and waste emission for the solar-assisted chemical brushing process and $NaClO_2$ solution–based delignification process. (**E**) A radar plot showing a comparison of the fabrication process for transparent wood. Photo credit: Qinqin Xia, University of Maryland, College Park.

immersed into adequate chemicals for an effective reaction, causing large amounts of chemical consumption and waste disposal. From the energy/chemical consumption point-of-view, the transparent wood fabricated by solar-assisted chemical brushing approach features greatly reduced energy (solar versus electrical heating) and chemical costs (3.14 versus 7.31 $/kg) compared to the lignin-removed transparent wood. From the waste emission point-of-view, our transparent wood also generates much less waste liquid (30 versus 960 ml) and no toxic gas (0 versus 960 ml). Thus, compared with the traditional solution-based delignification methods, the solar-assisted chemical brushing technique can produce transparent wood with the following advantages (Fig. 5E): (i) fast, low-cost, sustainable, and scalable fabrication; (ii) high lignin retention (~81%); and (iii) patternable transparent features.

In summary, we demonstrate a rapid, cost-effective, and sustainable method to fabricate patternable transparent wood based on a scalable solar-assisted chemical brushing method. In this process, the light-absorbing chromophore groups of lignin were removed, which allowed us to improve the optical properties of the resulting transparent wood without destroying the aromatic structure of lignin entirely. Both the longitudinally and transversely cut transparent wood with a thickness of ~1 mm show a high tensile strength of 31.4 to 46.2 MPa, excellent optical transmittance of >90%, low optical absorption of <4%, and high optical haze of 60 to 80%. This transparent wood demonstrates excellent optical properties without significantly sacrificing the material's mechanical strength due to the high lignin preservation. Moreover, the solar-assisted chemical brushing method can selectively treat designated areas of wood samples, imparting the transparent wood with excellent designable patterning capabilities. Compared to solution-based delignification processes, our solar-assisted chemical brushing has higher production efficiency, lower cost, and is more sustainable and controllable. This inexpensive and highly efficient fabrication of transparent wood can also use natural solar energy, expanding the technique's application to large-scale industrial production.

MATERIALS AND METHODS

Materials and chemicals

American balsa wood with the density of 0.15 to 0.26 g/cm^3 was purchased from Specialized Balsa Wood LLC. Sodium hydroxide

(NaOH) (Carolina Biological Supply Company), hydrogen peroxide (H_2O_2, 30% solution; EMD Millipore Corporation), and UV lamp (380 to 395 nm of wavelength; China) were used for lignin modification of the balsa wood. The epoxy resin (#300 resin and #21 Non Blushing Cycloaliphatic Hardener, AeroMarine Products Inc.) was further used for infiltration.

Fabrication of the transparent wood

A balsa wood log was cut along the transverse and longitudinal directions to form wood slices (0.6 to 3.3 mm in thickness). Then, the wood slices were brushed H_2O_2 (30 wt %), followed by UV illumination until the samples became completely white. We used a UV lamp (380 to 395 nm of wavelength) to simulate UV light in solar radiation. Note that a trace amount of NaOH (10 wt %) was coated on the wood surface before brushing H_2O_2 to improve the oxidation efficiency of the H_2O_2. This process removes the chromophores in lignin, causing the color of the wood to change from brown to white. The treated wood pieces were then immersed in ethanol for 5 hours to remove any remaining chemicals and then transferred to toluene so as to exchange the ethanol in the wood. Later, the samples were impregnated with epoxy (AeroMarine 300/21 epoxy) by vacuum infiltration for 1.5 hours. Last, the epoxy-impregnated wood samples were stored at room temperature until the epoxy was completely cured.

Fabrication process of the lignin-removed wood

$NaClO_2$ was added into water to prepare a 5% solution, followed by the addition of acetic acid to change the pH to ~4.6. The natural wood was immersed in this boiling $NaClO_2$ solution for 8 hours until the samples became completely white.

Characterization

The morphologies of the natural wood, lignin-modified wood, and transparent wood were observed on an SEM (Hitachi SU-70). FTIR spectra were recorded using a Nexus 670 FTIR Spectrometer over the range of 650 to 4000 cm^{-1}.

The x-ray photoelectron spectroscopy (XPS) experiments were calibrated by the binding energy of C1s as a reference of 284.6 eV. Eclipse V2.1 data analysis software supplied by the VG ESCA-Lab200I-XL instrument manufacturer was applied in the manipulation of the acquired XPS spectra.

The content of lignin (Klason lignin) in wood samples was measured according to TAPPI method (*45*). First, 0.1-g lignin-modified wood was reacted with 1.5 ml of 72% H_2SO_4 at room temperature with stirring for 2 hours. Second, the solution was diluted with deionized water to a 3% H_2SO_4 concentration and refluxed for 4 hours. Last, the mixture was filtered by sand core funnel, and the acid-insoluble lignin was determined by gravimetric analysis. The percentage of acid-insoluble lignin presents the content of the preserved modified lignin. Three samples of each material were tested to obtain the averaged values.

The optical spectra, including absorption, transmittance, and haze, were measured by a UV-Vis Spectrometer Lambda 35 (PerkinElmer, USA). An integrated sphere was used to collect the reflected and transmitted light. The dimensions of the natural wood and lignin-modified wood used for optical test were approximately 60 mm by 60 mm by 1 mm. The dimensions of transparent wood along the longitudinal and transverse directions used for optical test were approximately 60 mm by 60 mm by 1 mm, respectively. Note that multiple samples of transparent wood, lignin-modified wood, and natural wood were tested.

Mechanical tensile testing

The tensile properties of the natural wood, lignin-modified wood, lignin-removed wood, and transparent wood samples were measured using a Tinius Olsen H5KT tester. Five experiments were carried out for each sample. The dimensions of the samples were approximately 50 mm by 5 mm by (0.8 to 1.4) mm. The samples were stretched along the longitudinal and transverse directions of the wood until they fractured with a constant test speed of 5 mm min^{-1}.

The volume fraction of lignin-modified wood

The volume fraction of lignin-modified wood in the transparent wood was calculated according to the following equations (*46*)

$$V_f = \frac{W_f x \rho_c}{\rho_f} \quad (1)$$

$$\rho_c = 1/\left(\frac{W_f}{\rho_f} + \frac{W_m}{\rho_m}\right) \quad (2)$$

where V_f is the volume fraction of lignin-modified wood, ρ_c is the density of composite, ρ_m is the density of epoxy (1.09 g/cm^3), ρ_f is the density of lignin-modified wood (~0.2 g/cm^3), W_f is the weight fraction of lignin-modified wood, and W_m is the weight fraction of the epoxy.

SUPPLEMENTARY MATERIALS

Supplementary material for this article is available at http://advances.sciencemag.org/cgi/content/full/7/5/eabd7342/DC1

REFERENCES AND NOTES

1. M. M. Hossain, B. Jia, M. Gu, A metamaterial emitter for highly efficient radiative cooling. *Adv. Opt. Mater.* **3**, 1047–1051 (2015).
2. X. Zhao, H. Zhou, V. S. Sikarwar, M. Zhao, A.-H. A. Park, P. S. Fennell, L. Shen, L.-S. Fan, Biomass-based chemical looping technologies: The good, the bad and the future. *Energ. Environ. Sci.* **10**, 1885–1910 (2017).
3. X. P. Zhao, S. A. Mofid, T. Gao, G. Tan, B. P. Jelle, X. B. Yin, R. G. Yang, Durability-enhanced vanadium dioxide thermochromic film for smart windows. *Mater. Today Phys.* **13**, 100205 (2020).
4. M. Ono, M. Hata, M. Tsunekawa, K. Nozaki, H. Sumikura, H. Chiba, M. Notomi, Ultrafast and energy-efficient all-optical switching with graphene-loaded deep-subwavelength plasmonic waveguides. *Nat. Photonics* **14**, 37–43 (2020).
5. Y. J. Tan, H. Godaba, G. Chen, S. T. M. Tan, G. Wan, G. Li, P. M. Lee, Y. Cai, S. Li, R. F. Shepherd, J. S. Ho, B. C. K. Tee, A transparent, self-healing and high-κ dielectric for low-field-emission stretchable optoelectronics. *Nat. Mater.* **19**, 182–188 (2020).
6. Y. Liu, S.-H. Yu, L. Bergström, Transparent and flexible nacre-like hybrid films of aminoclays and carboxylated cellulose nanofibrils. *Adv. Funct. Mater.* **28**, 1703277 (2018).
7. Z. Sun, A. Martinez, F. Wang, Optical modulators with 2D layered materials. *Nat. Photonics* **10**, 227–238 (2016).
8. M. Li, Q. Zhao, S. Zhang, D. G. Li, H. Li, X. Zhang, B. Xing, Facile passivation of black phosphorus nanosheets via silica coating for stable and efficient solar desalination. *Environ. Sci. Nano* **7**, 414–423 (2020).
9. H. S. Yaddanapudi, N. Hickerson, S. Saini, A. Tiwari, Fabrication and characterization of transparent wood for next generation smart building applications. *Vacuum* **146**, 649–654 (2017).
10. Y. Li, Q. Fu, X. Yang, L. Berglund, Transparent wood for functional and structural applications. *Philos. Trans. R. Soc. A* **376**, 20170182 (2018).
11. C. Chen, Y. Kuang, S. Zhu, I. Burgert, T. Keplinger, A. Gong, T. Li, L. Berglund, S. J. Eichhorn, L. Hu, Structure–property–function relationships of natural and engineered wood. *Nat. Rev. Mater.* **5**, 642–666 (2020).
12. J. H. Pikul, S. Özerinç, B. Liu, R. Zhang, P. V. Braun, V. S. Deshpande, W. P. King, High strength metallic wood from nanostructured nickel inverse opal materials. *Sci. Rep.* **9**, 719 (2019).

13. M. Zhu, T. Li, C. S. Davis, Y. Yao, J. Dai, Y. Wang, F. AlQatari, J. W. Gilman, L. Hu, Transparent and haze wood composites for highly efficient broadband light management in solar cells. *Nano Energy* **26**, 332–339 (2016).
14. T. Li, M. Zhu, Z. Yang, J. Song, J. Dai, Y. Yao, W. Luo, G. Pastel, B. Yang, L. Hu, Wood composite as an energy efficient building material: Guided sunlight transmittance and effective thermal insulation. *Adv. Energy Mater.* **6**, 1601122 (2016).
15. C. F. Guo, Z. Ren, Flexible transparent conductors based on metal nanowire networks. *Mater. Today* **18**, 143–154 (2015).
16. A. Cannavale, P. Cossari, G. E. Eperon, S. Colella, F. Fiorito, G. Gigli, H. J. Snaith, A. Listorti, Forthcoming perspectives of photoelectrochromic devices: A critical review. *Energ. Environ. Sci.* **9**, 2682–2719 (2016).
17. J. Du, S. Pei, L. Ma, H.-M. Cheng, 25th anniversary article: Carbon nanotube- and graphene-based transparent conductive films for optoelectronic devices. *Adv. Mater.* **26**, 1958–1991 (2014).
18. W. Gan, S. Xiao, L. Gao, R. Gao, J. Li, X. Zhan, Luminescent and transparent wood composites fabricated by poly(methyl methacrylate) and γ-Fe_2O_3@YVO_4:Eu^{3+} nanoparticle impregnation. *ACS Sustain. Chem. Eng.* **5**, 3855–3862 (2017).
19. Z. Yu, Y. Yao, J. Yao, L. Zhang, Z. Chen, Y. Gao, H. Luo, Transparent wood containing Cs_xWO_3 nanoparticles for heat-shielding window applications. *J. Mater. Chem. A* **5**, 6019–6024 (2017).
20. L. Wang, Y. Liu, X. Zhan, D. Luo, X. Sun, Photochromic transparent wood for photo-switchable smart window applications. *J. Mater. Chem. C* **7**, 8649–8654 (2019).
21. Q. Xue, R. Xia, C. J. Brabec, H.-L. Yip, Recent advances in semi-transparent polymer and perovskite solar cells for power generating window applications. *Energ. Environ. Sci.* **11**, 1688–1709 (2018).
22. C.-C. Chen, L. D. Dou, R. Zhu, C.-H. Chung, T.-B. Song, Y. B. Zheng, S. Hawks, G. Li, P. S. Weiss, Y. Yang, Visibly transparent polymer solar cells produced by solution processing. *ACS Nano* **6**, 7185–7190 (2012).
23. C.-C. Kim, H.-H. Lee, K. H. Oh, J.-Y. Sun, Highly stretchable, transparent ionic touch panel. *Science* **353**, 682–687 (2016).
24. M. Wang, R. Li, G. Chen, S. Zhou, X. Feng, Y. Chen, M. He, D. Liu, T. Song, H. Qi, Highly stretchable, transparent, and conductive wood fabricated by in situ photopolymerization with polymerizable deep eutectic solvents. *ACS Appl. Mater. Interfaces* **11**, 14313–14321 (2019).
25. Y. Li, Y. Liu, W. Chen, Q. Wang, Y. Liu, J. Li, H. Yu, Facile extraction of cellulose nanocrystals from wood using ethanol and peroxide solvothermal pretreatment followed by ultrasonic nanofibrillation. *Green Chem.* **18**, 1010–1018 (2016).
26. E. Vasileva, H. Chen, Y. Li, I. Sychugov, M. Yan, L. Berglund, S. Popov, Light scattering by structurally anisotropic media: A benchmark with transparent wood. *Adv. Opt. Mater.* **6**, 1800999 (2018).
27. M. Frey, D. Widner, J. S. Segmehl, K. Casdorff, T. Keplinger, I. Burgert, Delignified and densified cellulose bulk materials with excellent tensile properties for sustainable engineering. *ACS Appl. Mater. Interfaces* **10**, 5030–5037 (2018).
28. Q. Fu, M. Yan, E. Jungstedt, X. Yang, Y. Li, L. A. Berglund, Transparent plywood as a load-bearing and luminescent biocomposite. *Compos. Sci. Technol.* **164**, 296–303 (2018).
29. H. Guan, Z. Cheng, X. Wang, Highly compressible wood sponges with a spring-like lamellar structure as effective and reusable oil absorbents. *ACS Nano* **12**, 10365–10373 (2018).
30. J. Qin, X. Li, Y. Shao, K. Shi, X. Zhao, T. Feng, Y. Hu, Optimization of delignification process for efficient preparation of transparent wood with high strength and high transmittance. *Vacuum* **158**, 158–165 (2018).
31. J. Wu, Y. Wu, F. Yang, C. Tang, Q. Huang, J. Zhang, Impact of delignification on morphological, optical and mechanical properties of transparent wood. *Compos. Part A Appl. Sci. Manuf.* **117**, 324–331 (2019).
32. A. N. Subba Rao, G. B. Nagarajappa, S. Nair, A. M. Chathoth, K. K. Pandey, Flexible transparent wood prepared from poplar veneer and polyvinyl alcohol. *Compos. Sci. Technol.* **182**, 107719 (2019).
33. H. Zhang, Y. Bai, W. Zhou, F. Chen, Color reduction of sulfonated eucalyptus kraft lignin. *Int. J. Biol. Macromol.* **97**, 201–208 (2017).
34. Y. Qian, Y. Deng, H. Li, X. Qiu, Reaction-free lignin whitening via a self-assembly of acetylated lignin. *Ind. Eng. Chem. Res.* **53**, 10024–10028 (2014).
35. Y. Qin, D. Yang, X. Qiu, Hydroxypropyl sulfonated lignin as dye dispersant: Effect of average molecular weight. *ACS Sustain. Chem. Eng.* **3**, 3239–3244 (2015).
36. Y. Li, Q. Fu, R. Rojas, M. Yan, M. Lawoko, L. Berglund, Lignin-retaining transparent wood. *ChemSusChem* **10**, 3445–3451 (2017).
37. M. Herrera, K. Thitiwutthisakul, X. Yang, P.-o. Rujitanaroj, R. Rojas, L. Berglund, Preparation and evaluation of high-lignin content cellulose nanofibrils from eucalyptus pulp. *Cellulose* **25**, 3121–3133 (2018).
38. Z. Shi, G. Xu, J. Deng, M. Dong, V. Murugadoss, C. Liu, Q. Shao, S. Wu, Z. Guo, Structural characterization of lignin from *D. sinicus* by FTIR and NMR techniques. *Green Chem. Lett. Rev.* **12**, 235–243 (2019).
39. Z. Jiang, J. Yi, J. Li, T. He, C. Hu, Promoting effect of sodium chloride on the solubilization and depolymerization of cellulose from raw biomass materials in water. *ChemSusChem* **8**, 1901–1907 (2015).
40. Z.-L. Yu, N. Yang, L.-C. Zhou, Z.-Y. Ma, Y.-B. Zhu, Y.-Y. Lu, B. Qin, W.-Y. Xing, T. Ma, S.-C. Li, H.-L. Gao, H.-A. Wu, S.-H. Yu, Bioinspired polymeric woods. *Sci. Adv.* **4**, eaat7223 (2018).
41. J. Song, C. Chen, S. Zhu, M. Zhu, J. Dai, U. Ray, Y. Li, Y. Kuang, Y. Li, N. Quispe, Y. Yao, A. Gong, U. H. Leiste, H. A. Bruck, J. Y. Zhu, A. Vellore, H. Li, M. L. Minus, Z. Jia, A. Martini, T. Li, L. Hu, Processing bulk natural wood into a high-performance structural material. *Nature* **554**, 224–228 (2018).
42. Y. Li, E. Vasileva, I. Sychugov, S. Popov, L. Berglund, Optically transparent wood: Recent progress, opportunities, and challenges. *Adv. Opt. Mater.* **6**, 1800059 (2018).
43. G. Jacucci, L. Schertel, Y. Zhang, H. Yang, S. Vignolini, Light management with natural materials: From whiteness to transparency. *Adv. Mater.*, 2001215 (2020).
44. A. Coffey, M. A. K. Jansen, Effects of natural solar UV-B radiation on three Arabidopsis accessions are strongly affected by seasonal weather conditions. *Plant Physiol. Biochem.* **134**, 64–72 (2019).
45. TAPPI, T 222 om-02: Acid-insoluble lignin in wood and pulp. *2002–2003 TAPPI Test Methods* (2002).
46. Y. Li, Q. Fu, S. Yu, M. Yan, L. Berglund, Optically transparent wood from a nanoporous cellulosic template: Combining functional and structural performance. *Biomacromolecules* **17**, 1358–1364 (2016).

Acknowledgments

Funding: We acknowledge support of the A. James & Alice B. Clark Foundation and the A. James School of Engineering at the University of Maryland. **Author contributions:** L.H., Q.X., C.C., and T.L. designed the experiments. Q.X. conducted the experiments and carried out the characterization. Q.X., C.C., and S.H. analyzed the data. J.G. and X.W. collected photographs of transparent wood. L.H., Q.X., and C.C. collaboratively wrote the paper. All authors commented on the final manuscript. **Competing interests:** L.H., Q.X., T.L., and C.C. are inventors on a patent application related to this work filed by University of Maryland, College Park (U.S. Provisional Application No.: PS-2019-110, filing date: 10 July 2020) titled "Patterned transparent wood composite structure and use thereof." All other authors declare that they have no competing interests. **Data and materials availability:** All data needed to evaluate the conclusions in the paper are present in the paper and/or the Supplementary Materials. Additional data related to this paper may be requested from the authors.

Submitted 9 July 2020
Accepted 10 December 2020
Published 27 January 2021
10.1126/sciadv.abd7342

Citation: Q. Xia, C. Chen, T. Li, S. He, J. Gao, X. Wang, L. Hu, Solar-assisted fabrication of large-scale, patternable transparent wood. *Sci. Adv.* **7**, eabd7342 (2021).